BRACETS: Bimodal repository of auscultation coupled with electrical impedance thoracic signals

Diogo Pessoa [a,*], Bruno Machado Rocha [a], Claas Strodthoff [b], Maria Gomes [c], Guilherme Rodrigues [c], Georgios Petmezas [d], Grigorios-Aris Cheimariotis [d], Vassilis Kilintzis [d], Evangelos Kaimakamis [e], Nicos Maglaveras [d], Alda Marques [c,f], Inéz Frerichs [b], Paulo de Carvalho [a], Rui Pedro Paiva [a]

[a] University of Coimbra Centre for Informatics and Systems of the University of Coimbra, Department of Informatics Engineering, 3030-290 Coimbra, Portugal
[b] Department of Anesthesiology, and Intensive Care Medicine, University Medical Center Schleswig-Holstein Campus Kiel, Kiel 24105, Schleswig-Holstein, Germany
[c] Lab3R - Respiratory Research and Rehabilitation Laboratory, School of Health Sciences (ESSUA), University of Aveiro, 3810-193 Aveiro, Portugal
[d] 2nd Department of Obstetrics and Gynaecology, The Medical School, 54124 Thessaloniki, Greece
[e] 1st Intensive Care Unit, "G. Papanikolaou" General Hospital of Thessaloniki, 57010 Pilea Hortiatis, Greece
[f] Institute of Biomedicine (iBiMED), University of Aveiro, 3810-193 Aveiro, Portugal

ARTICLE INFO

ABSTRACT

Background and Objective: Respiratory diseases are among the most significant causes of morbidity and mortality worldwide, causing substantial strain on society and health systems. Over the last few decades, there has been increasing interest in the automatic analysis of respiratory sounds and electrical impedance tomography (EIT). Nevertheless, no publicly available databases with both respiratory sound and EIT data are available. Methods: In this work, we have assembled the first open-access bimodal database focusing on the differential diagnosis of respiratory diseases (BRACETS: Bimodal Repository of Auscultation Coupled with Electrical Impedance Thoracic Signals). It includes simultaneous recordings of single and multi-channel respiratory sounds and EIT. Furthermore, we have proposed several machine learning-based baseline systems for automatically classifying respiratory diseases in six distinct evaluation tasks using respiratory sound and EIT (A1, A2, A3, B1, B2, B3). These tasks included classifying respiratory diseases at sample and subject levels. The performance of the classification models was evaluated using a 5-fold cross-validation scheme (with subject isolation between folds). Results: The resulting database consists of 1097 respiratory sounds and 795 EIT recordings acquired from 78 adult subjects in two countries (Portugal and Greece). In the task of automatically classifying respiratory diseases, the baseline classification models have achieved the following average balanced accuracy: Task A1 - 77.9±13.1%; Task A2 - 51.6±9.7%; Task A3 - 38.6±13.1%; Task B1 - 90.0±22.4%; Task B2 - 61.4±11.8%; Task B3 - 50.8±10.6%. Conclusion: The creation of this database and its public release will aid the research community in developing automated methodologies to assess and monitor respiratory function, and it might serve as a benchmark in the field of digital medicine for managing respiratory diseases. Moreover, it could pave the way for creating multi-modal robust approaches for that same purpose.

1. Introduction

Respiratory diseases are among the most significant causes of morbidity and mortality worldwide and are responsible for a substantial strain on individuals, healthcare systems, and society [1,2]. Early diagnosis and frequent monitoring are essential for the management of these patients. Currently, chronic respiratory diseases are not curable; however, various pharmacological (e.g., bronchodilators) and non-pharmacological (e.g., physical activity, pulmonary rehabilitation) treatments contribute to improve the symptoms (e.g., shortness of breath, fatigue), physical and emotional status, and quality of life of patients with such diseases. Nevertheless, early diagnosis, detection of acute exacerbation (defined as an acute worsening of respiratory symptoms that result in additional therapy [3]), and long-term

---

management remain highly challenging and have led to significant research efforts to improve the prognosis of these conditions.

Respiratory medicine diagnosis relies on clinical information and complementary laboratory test results [4]. Two of the most commonly used examination procedures in standard clinical practice for the diagnosis of respiratory diseases are respiratory sound auscultation and spirometry [5]. The auscultation of the respiratory system is one of the oldest techniques to diagnose various pulmonary diseases [6]. It is an inexpensive, noninvasive, safe, and easy-to-perform technique. Even though auscultation is a versatile and easy-to-deploy examination technique, it has intrinsic limitations, such as inter-listener variability and subjectivity [7]. Moreover, the examination must be performed face-to-face.

On the other hand, spirometry is a physiological test that measures how an individual inhales or exhales volumes of air as a function of time [8]. One of the significant advantages of this test is that it has well-established normality values. It is well-validated in diagnosing and monitoring airway and lung parenchyma abnormalities [5]. However, it highly depends on the cooperation between the technician and the patient, with results greatly influenced by technical factors and patient effort [5].

Respiratory medicine also relies heavily on diagnostic techniques, such as chest radiography, computed tomography (CT), and tissue biopsies, among others. These techniques are generally more expensive, require more complex setups, and can be invasive, unlike auscultation and spirometry.

One of the most active research areas in respiratory function assessment has been the computerized analysis of respiratory sound. The main objective of this computerized approach is to overcome the drawbacks of conventional methods and provide more objective measures to monitor and diagnose patients suffering from lung diseases. Some drawbacks of conventional auscultation include its subjectivity in interpretation and difficulties memorizing findings from different chest locations and overtime. Computerized respiratory sound analysis (CORSA), which consists of recording patients' respiratory sounds with an electronic device and analyzing them based on specific signal characteristics, is a simple, objective, and noninvasive method to detect and characterize respiratory sound in general, with particular emphasis on adventitious respiratory sounds (ARSs) [9]. ARSs are additional respiratory sounds superimposed on normal respiratory sounds. They can be continuous (like wheezes) or discontinuous (such as crackles). Their presence usually indicates pulmonary disorders [10]. Moreover, with the advances in embedded processors developed with low power consumption battery technology and integrated sensors to make stethoscopes wearable and wireless, CORSA are also suitable to be deployed in remote applications [7,11,12]. Since the COVID-19 outbreak, remote monitoring has become a pressing need, primarily for sanitary reasons [13]. Therefore, automated methods for analyzing respiratory sounds are increasingly needed to reliably carry out remote auscultation and monitoring of subjects suffering from respiratory diseases.

Another technique for monitoring the respiratory system that has experienced significant development in recent years is electrical impedance tomography (EIT). EIT is a radiation-free imaging technique that uses low electrical currents to determine differences in electrical impedance (or conductivity) and generate cross-sectional images of impedance distribution within electrically conductive objects (e.g., the chest region) [14,15]. In its simplest form, EIT is accomplished by placing electrodes on the surface of the body and passing current between two electrodes while measuring the voltages induced on the remaining electrodes. Then, an inverse calculation is performed from these measurements to determine conductivity changes across the section being measured [15].

In the clinical application, EIT has emerged as a noninvasive, bedside monitoring technique that provides continuous, real-time information about the regional distribution of changes in the electrical resistivity of lung tissue due to variations in ventilation (or blood flow/perfusion) in relation to a reference state [16]. Besides that, thoracic EIT has also been extensively used for monitoring subjects under mechanical ventilation and pulmonary function testing [17]. Previous clinical studies have supported the validity and reproducibility of EIT findings by comparing them against reference techniques such as CT-scan, single-photon emission CT, positron emission tomography, vibration response imaging, inert-gas washout, and spirometry [17].

Despite being primarily used in hospitals, several studies in the literature have proposed/used wearable EIT systems in other settings [14,18–24]. The main goal of such systems is their deployment in telehealth/digital health applications for the remote monitoring of subjects suffering from respiratory diseases. Thus, similar to what happens with CORSA, there is also a growing need to develop automated methods using EIT to remotely monitor patients.

One of the core problems in the field of automated respiratory function analysis is the need for large publicly available databases that can serve to develop algorithms and benchmark results [25]. Having large and representative databases is an essential requirement for algorithmic development as well as accurate and robust diagnostics. Otherwise, it is hard to develop methods with good generalization capacity that perform well in real-world conditions.

Over the last decades, many studies have targeted the development of methods for the automatic processing of respiratory sounds (especially adventitious respiratory sounds) [26]. Most of these works were based on traditional signal processing and machine learning approaches, with a reduced number of works using shallow neural networks. Most of them were based on a small number of subjects and respiratory sound recordings. Table 1 summarizes the current publicly available databases on respiratory sound. Unlike the more recent online repositories (the last seven rows in Table 1), the older databases were typically designed for teaching purposes, with fewer samples available, and primarily collected in controlled environments.

In general, most of the available databases listed in Table 1 were curated to be used in developing algorithms to process adventitious respiratory sounds. Only the databases presented in [39–42] can also be used to develop methods for the classification/detection of respiratory diseases. In clinical practice, physicians typically use various methods to diagnose respiratory diseases, such as spirometry, lung auscultation, and CT-scan, among other techniques [25]. So far, respiratory sound has been commonly used in the literature for developing models, typically machine learning based, for classifying respiratory diseases [25]. The databases from [39,40,42] have been commonly used to tackle this problem. A selection of works on respiratory disease classification through automated auscultation is summarized in Table 2.

Despite the high results reported for the automatic classification of respiratory diseases, there is still significant room for improvement before these methods can be deployed in real-world applications. One key area that must be addressed is the evaluation of the generalization capability of the developed models, that is, the validation of the models with different databases. This is a critical step to understanding the validity of the proposed methods in new scenarios (i.e., different subjects, recording environment, and recording equipment, among others). However, it is hard to accomplish such validation due to the reduced number of databases in the area.

Another main point that must be carefully addressed is related to the validation scheme of the developed models. For instance, the RSD [39, 40] uses a one-time subject-independent hold-out separation mechanism to divide the database into training and testing. Likewise, many studies using this database (or other) follow the same approach. This approach might lead to overly optimistic results since only a small portion of subjects is used to evaluate the performance of the developed algorithms, introducing significant bias. This may be observed in several works [47,48,50,51] presented in Table 2. Another common problem in the literature is the lack of subject separation between the training and testing sets. Authors often consider a cross-validation scheme to evaluate their models but do not ensure subject isolation between sets [49,

Table 1

List of publicly available respiratory sound databases.

Database name and reference	Number of subjects	Number of recordings	Type
The Chest: its Signs and Sounds [27]	-	-	CD
Understanding Lung Sounds, second edition and third edition [28,29]	-	28	CD
Understanding Heart Sounds and Murmurs [30]	-	-	CD
R.A.L.E. repository [31]	-	>50	Online repository
East Tennessee State University repository [32]	-	20	Online repository
Fundamentals of Lung and Heart Sounds [33]	-	-	CD
Auscultation Skills: Breath and Heart Sounds, fourth edition [34]	-	96	CD
Heart and lung sounds reference library [35]	-	46	CD
Lung Sounds: An Introduction to the Interpretation of the Auscultatory Findings [36]	-	28	CD
Secrets Heart & Lung Sounds Workshop [37]	-	-	CD
SoundCloud Lung Sound repository [38]	-	-	Online repository
ICBHI 2017/Respiratory Sound Database (RSD) [39,40]	126	920	Online repository
RespiratoryDatabase@TR (COPD Severity Analysis) [41]	75	504	Online repository
A dataset of lung sounds recorded from the chest wall using an electronic stethoscope [42]	112	112	Online repository
HF_Lung_V1 [43]	261	9765	Online repository
HF_Lung_V2 [44]	300	13,957	Online repository
HF_Tracheal_V1 [45]	227	10,448	Online repository
SPRSound: Open-Source SJTU Paediatric Respiratory Sound Database [46]	292	2683	Online repository

52]. Once again, significant bias was introduced in the evaluation of the methods with such approaches.

Unlike respiratory sound, EIT has not been widely explored in the development of automated classification methodologies of respiratory diseases. In a preliminary study using part of the BRACETS database, several machine learning models have been proposed to automatically classify isolated respiratory cycles from healthy and non-healthy subjects using EIT [56]. In another study [57], the authors proposed a model to classify apnea and non-apnea cases in neonatal patients using EIT. A ResNet50 was used to encode features from the EIT data, which were then fed to an SVM classification model. Lastly, EIT image sequences have also been used with deep learning methods in an end-to-end fashion to estimate respiratory and circulatory parameters (normalized blood pressure, normalized airway pressure, absolute flow, and absolute volume) [58].

To the best of our knowledge, thoracic EIT has no large open-access databases. Open-access EIT data are typically available for demonstration/education purposes, with a reduced number of samples. Moreover, we are unaware of any public database containing combined respiratory sound and EIT data.

The main objective of this work was to establish the first open-access bimodal database (respiratory sound and EIT) for purposes of respiratory disease diagnosis. Secondary aims included sharing a mechanism that allows the synchronization of recordings from respiratory sound and EIT during post-processing and proposing several machine-learning models for the automated classification of respiratory diseases based on the current database. In summary, the main contributions of this work are the following:

1. Establishment of the first bimodal (respiratory sound + EIT) open-access database for the diagnosis of respiratory diseases (https://data.mendeley.com/datasets/f43c7snks5/1);
2. Proposal of a benchmark machine learning pipeline for the classification of respiratory diseases using the current database (traditional machine learning and deep learning models);
3. Use of EIT for the development of automated classification models of respiratory diseases;

Table 2

Summary of selected works on respiratory disease classification. (CNN - convolutional neural network; LSTM - long short-term memory; ConvBiGRNN - convolutional bidirectional gated recurrent neural network; NMF - Non-negative matrix factorization; F1 - F1 score; HS - harmonic score).

Reference	Data	Method	Classes	Best Results (%)
Aykanat et al. [47]	*Participants*: 1630; *Recordings*: 17930; *Source*: Private	CNN	Healthy; Unhealthy	*Accuracy*: 85; *Precision*: 86; *Sensitivity*: 86; *Specificity*: 86
Perna et al. [48]	*Participants*: 126; *Recordings*: 920; *Source*: RSD	RNN	Healthy; Chronic; Non-chronic	*Accuracy*: 98; *Precision*: 93; *Sensitivity*: 90; *Specificity*: 82; *F1*: 91
Garcia-Ordás et al. [49]	*Participants*: 126; *Recordings*: 920; *Source*: RSD	Autoencoder + CNN	(1) Healthy; Chronic; Non-chronic, (2) URTI; COPD; Bronchiectasis; Pneumonia; Bronchiolitis; Healthy	(1) - *F1*: 99; (2) - *F1*: 99
Shuvo et al. [50]	*Participants*: 126; *Recordings*: 920; *Source*: RSD	CNN	(1) Healthy; Chronic; Non-chronic, (2) URTI; COPD; Bronchiectasis; Pneumonia; Bronchiolitis; Healthy	(1) - *Accuracy*: 98.7; *Sensitivity*: 98.9; *Specificity*: 100, (2) - *Accuracy*: 98.7; *Sensitivity*: 98.6; *Specificity*: 100
Torre-Cruz et al. [51]	*Participants*: 208; *Recordings*: 208; *Source*: Public	Semi-supervised NMF	Healthy; Unhealthy	*Accuracy*: 96; *Precision*: 100; *Sensitivity*: 93; *Specificity*: 100
Fraiwan et al. [52]	*Participants*: 215; *Recordings*: 1484; *Source*: RSD and King Abdullah University Hospital Dataset	Ensemble Classifiers	Healthy; Asthma; COPD; Bronchiectasis; Pneumonia; Heart failure	*Accuracy*: 98.27; *Sensitivity*: 95.28; *Specificity*: 98.9; *F1*: 93.61
Fraiwan et al. [53]	*Participants*: 215; *Recordings*: 1484; *Source*: RSD and King Abdullah University Hospital Dataset	CNN + LSTM	Healthy; Asthma; COPD; Bronchiectasis; Pneumonia; Heart failure	*Accuracy*: 99.62; *Sensitivity*: 98.43; *Specificity*: 99.79
Messner et al. [54]	*Participants*: 23; *Recordings*: 387; *Source*: Private	ConvBiGRNN	Healthy; Pathological; No signal	*Precision*: 100; *Sensitivity*: 85.9; *F1*: 92.4
Nguyen et al. [55]	*Participants*: 215; *Recordings*: 387; *Source*: RSD and Private	ResNet50	(1) - Healthy; Chronic; Non-chronic, (2) - Healthy; Unhealthy	(1) *Specificity*: 91.77; *Sensitivity*: 93.68; *HS*: 92.57; (2) *Specificity*: 91.77; *Sensitivity*: 96.92; *HS*: 93.60

4. Development of an acquisition setup to allow data synchrony between respiratory sound and EIT.

2. Methods

2.1. Data collection protocol

In this section, we describe the data collection protocol. The study was conducted under the scope of the European Horizon 2020 project WELMO[1]. Furthermore, two independent ethics committees approved it in each country where the acquisitions took place: approval was granted by the Nursing School of Coimbra (ESEnfC) in Portugal (Reference AD1 P721-10/2020) and by the Scientific Council of General Papanikolaou Hospital in Greece (Reference 51st/252/4-3-2021). We have complied with all relevant ethical regulations. Informed written consent was obtained from all participants before examinations.

Respiratory sound data were recorded using the 3M Littmann Electronic Stethoscope 3200 with a sampling rate of 4000 Hz. The stethoscope was hand-held by a medical doctor/physiotherapist in the respective recording position. Recordings were either started using the stethoscope or the 3M Littmann StethAssist Software in an auxiliary computer. After recording the respiratory sound in every position considered, the recorded sounds were uploaded from the internal memory of the stethoscope to the auxiliary computer via Bluetooth. Every sound was then extracted from the StethAssist Software with the three available filtering modes: Bell, Diaphragm, and Extended. The Bell mode amplified sounds from 20 - 1000Hz, but emphasized lower frequency sounds between 20 - 200Hz; the Diaphragm mode amplified sounds from 20 - 2000Hz, but emphasized the sounds between 100 - 500Hz; the Extended Range mode amplified sounds from 20 - 2000Hz similar to the Diaphragm Mode, but provided more low-frequency response between 50 - 500Hz [59].

EIT data were collected using the Goe-MF II EIT device (CareFusion, Höchberg, Germany). An array of sixteen self-adhesive electrodes (Blue Sensor, Ambu, Ballerup, Denmark) was attached to the chest circumference between the 5-6th intercostal space (xiphoid-sternal line), with another reference electrode placed on the abdomen. Small alternating electrical currents (5 mA) were delivered through adjacent pairs of electrodes in a sequential rotating process, and the remaining passive electrode pairs measured the resulting potential differences. A total of 208 voltages were measured per image frame. EIT data were acquired at a sampling rate of 33 images/second (33 Hz).

A photographic register of the acquisition devices/setup is available in the supplementary material.

Data acquisitions took place in different countries using different acquisition protocols, namely the auscultation points differed between locations. Nevertheless, simultaneous acquisition of respiratory sound and electrical impedance tomography signals was performed in every subject. In summary, the main steps of the acquisition process can be summarized in the following key points:

- Dialogue with the participant providing instructions regarding the acquisition protocol and sequence of events;
- Placement of the EIT electrodes around the thoracic area (some subjects required the use of conductive gel);
- Recording of respiratory sounds at the various auscultation points and corresponding EIT signals (recordings at Aveiro contemplated an initial phase for post-acquisition data synchronization purposes);
- Removal of the EIT electrodes and storage of recorded respiratory sounds and EIT data to an external computer.

The recording points considered in each location as well as the number of respiratory sounds per location are presented in Fig. 1.

Below we present the protocols and the acquisition setups used at each location with further detail. Two types of acquisitions were collected in both locations. In the first type of acquisition (TbDb), most commonly used among clinicians during auscultation, participants performed tidal and deep breathing. In the second type (TbCS), participants were instructed to perform forced cough and speak to purposely introduce perturbations in the recordings.

2.1.1. School of Health Sciences, University of Aveiro (ESSUA)

Recordings were conducted by the research team of the Respiratory Research and Rehabilitation Laboratory (Lab3R) of the School of Health Sciences, University of Aveiro (ESSUA). Respiratory sounds were collected by placing an electronic stethoscope at five different positions (see Fig. 1). For each stethoscope placement, the corresponding EIT signal was also simultaneously recorded. Therefore, each acquisition comprised a pair of respiratory sound - EIT recordings. Participants were seated throughout the data collection process.

In the data collection process, two different types of acquisitions were performed. In the first type (tidal breathing + deep breathing - TbDb), subjects were requested to breathe quietly for a few seconds. After that period, they were prompted to start breathing deeply until the end of the recording. In the second type of acquisition (tidal breathing + cough + speech - TbCS), subjects were instructed to breathe quietly at first. After a couple of breaths, they were prompted to cough (intentionally) and speak (read a sentence shown by the respiratory therapists). The sentence was in Portuguese as follows: *"Está na hora de acabar"* (in English: "It is time to end"). This sentence was selected based on a previous study where several Portuguese phrases were submitted to an extensive acoustic analysis [60]. Both types of acquisitions were recorded for each recording position identified in Fig. 1. In Fig. 2, we present two example recordings with synchronized respiratory sound and EIT, one for each type of acquisition.

Since two independent devices were used for data collection (3M Littmann Electronic Stethoscope 3200 and Goe-MF II EIT device), the raw data from each source was not synchronized in the time domain. Therefore, we developed an acquisition setup using an auxiliary signal to synchronize respiratory sounds and EIT data in post-acquisition. The system generated an auxiliary sound signal (a pure sinusoidal tone at a specific frequency of 1900 Hz) that was then split to a loudspeaker and the EIT device, using an audio splitter and a 3.5 mm mono jack to BNC adapter (see Fig. 3). Accordingly, this division allowed the auxiliary signal to be simultaneously detected in both respiratory sound and EIT recording systems. Subsequently, both signals were synchronized post-acquisition by aligning the auxiliary signals in both sources.

The recording process was initiated with the EIT recording start, followed by the respiratory sound recording. The first seconds (approximately 10 seconds) after the sound recording was initiated were used to trigger the auxiliary input (see Fig. 3). The stethoscope was not in direct contact with the examined subject in this initial interval. This step was crucial to detect the auxiliary with the least attenuation possible. However, in the sounds recorded on the trachea (point 7 in Fig. 1), the stethoscope was in direct contact with the subjects the whole time, and the auxiliary signal was not audible in these cases. Since subjects usually experienced some level of discomfort at this specific auscultation point, we tried to place the stethoscope gently in the trachea and avoid the initial step of capturing the auxiliary signal over the sound. Therefore, for the sounds recorded over the trachea, it was not possible to detect the auxiliary signal in respiratory sound and, consequently, align the respiratory sound and EIT.

Fig. 4 represents the chronological sequence of events of the acquisitions. In this figure, we observe the auxiliary signal present in both EIT system auxiliary signal and respiratory sound. After the acquisition, we manually identified (for higher accuracy) the time intervals of the auxiliary signal in both signals. These intervals were later used to determine the *t1* interval (see Fig. 4) and align the respiratory sound and EIT recordings.
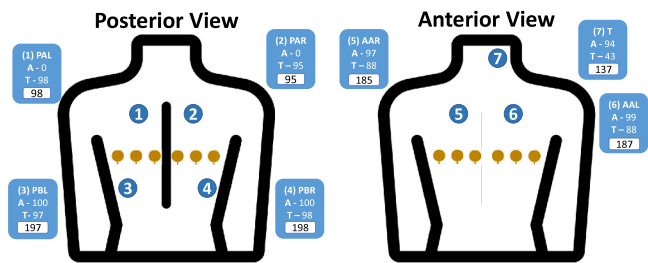

Fig. 1. Respiratory sound recording points (blue circles) and placement of EIT electrodes (yellow circles) during examinations. 1 - posterior apical left (PAL), 2 - posterior apical right (PAR), 3 - posterior basal left (PBL), 4 - posterior basal right (PBR), 5 - anterior apical right (AAR), 6 - anterior apical left (AAL), 7 - trachea (T). The blue rectangular shapes represent the number of recordings collected at each location at Aveiro (A), Thessaloniki (T), and in total (white rectangle). At Aveiro, only five auscultation points were considered (3,4,5,6,7).

2.1.2. Aristotle University of Thessaloniki (AUTH)

Respiratory sounds were acquired by the research team of the Aristotle University of Thessaloniki (AUTH) at the Geroge Papanikolaou General Hospital of Thessaloniki. Sounds were collected sequentially from six chest locations by simultaneously placing two electronic stethoscopes at two locations (multi-channel recording - not synchronized with EIT). The considered recording positions are presented in Fig. 1. The corresponding EIT signal was recorded for each pair of stethoscope placement. Therefore, each acquisition comprises a pair of two respiratory sounds - EIT recording. Participants were seated throughout the data collection process.

During the recordings, two different types of acquisitions were performed. In the first type (tidal breathing + deep breathing - TbDb), subjects were requested to breathe quietly for a few seconds. After that period, they were prompted to start breathing deeply. In the second type of acquisition (tidal breathing + cough + speech - TbCS), subjects were prompted to cough voluntarily, perform throat clearing, and, lastly, count from one to ten in greek: *"éna, dío, tría, tésera, pénde, éxi, eptá, októ, enéa, déka"*. Despite the slight differences in the protocol when compared to the recordings at Aveiro (subsubsection 2.1.1), the obtained samples were similar to the ones presented in Fig. 2.

Temporal data synchrony between respiratory sound and EIT was not ensured. Moreover, temporal synchrony between the respiratory sound of both stethoscopes was also not ensured. These were recorded with two independent devices without any external trigger to allow post-acquisition alignment. In the data collection process, the EIT recording was started first. Then, one of the health professionals collecting the respiratory sound with the stethoscope would signal the other to start the recording and initiate both stethoscopes simultaneously. Despite that, during the acquisitions, we verified that the second stethoscope was occasionally initiated with some delay (approximately 1 to 2 seconds).

2.2. Classification of respiratory diseases: Baseline

We have proposed a baseline system for classifying respiratory diseases based on respiratory sound and EIT data. This baseline will facilitate comparisons across future works using the current database.

In our baseline classification systems, we have considered a feature-level fusion [61], in which we merge features extracted from both respiratory sound and EIT. Moreover, we have also trained the same models with sound and EIT features separately.

Fig. 5 presents the overall pipeline of the proposed baseline classification models. It should be noted that for the samples recorded in Aveiro, there was only one respiratory sound available (single-channel recordings). Thus, only "Sample1" was considered for those cases. The extracted features were used to train and test the machine learning models.

2.2.1. Preprocessing

The acquired raw EIT data were processed offline to obtain the reconstructed images/frames using the Graz Consensus Reconstruction Algorithm for EIT (GREIT) [62]. The reconstruction was performed using an adult thorax-shaped model with a single plane of 16 electrodes. The adjacent stimulation pattern was selected from the library of models of the EIDORS software v3.10 [63]. The resulting reconstructed EIT images consisted of 32 by 32 pixels. After obtaining the reconstructed images for every time step (frame), the global EIT waveform was computed by summing up all individual pixel values for each complete image and multiple regions of interest (e.g., right part of the image, left part of the image, among others).

The initial 10 seconds of every recording were discarded for the respiratory sounds recorded in Aveiro since they were used for synchronization purposes. Thus, they might contain background noise unrelated to the respiratory sounds. Respiratory sounds used for the development of the differential diagnosis system were considered with
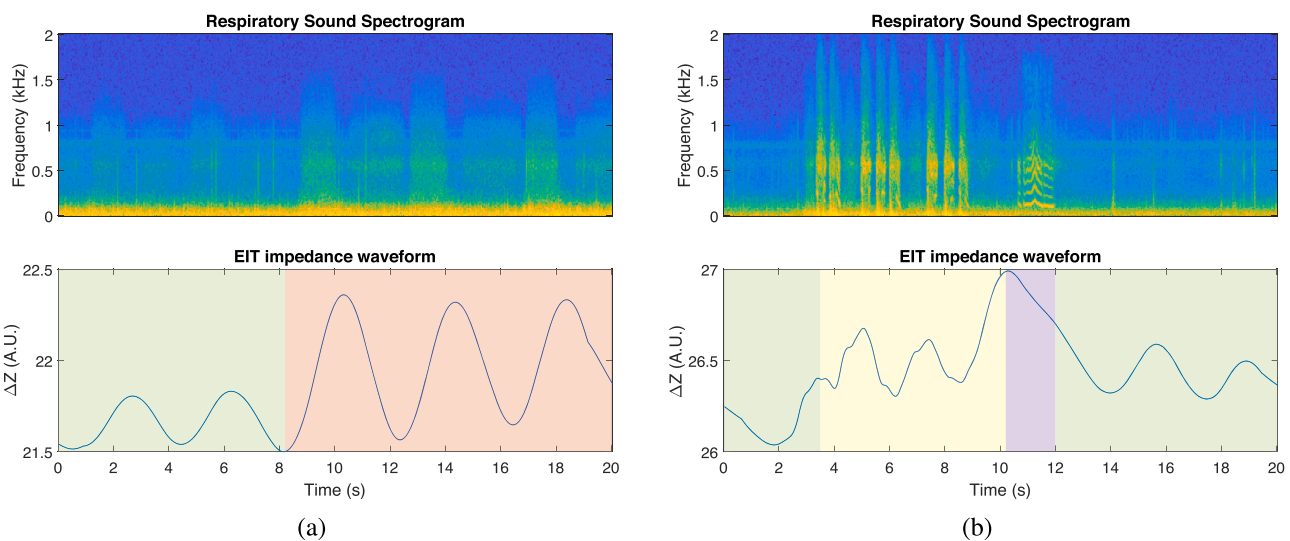

Fig. 2. Sample recording of each type of acquisition (TbDb from subject with COPD, and TbCS from subject with ILD). (a) TbDb acquisition: tidal breathing followed by deep breathing (green - tidal breathing; red - deep breathing); (b) TbCS acquisition: tidal breathing followed by forced cough and speech (green - tidal breathing; yellow - cough; purple - speech). (**ΔZ-impedance variation; A.U.-arbitrary units**).
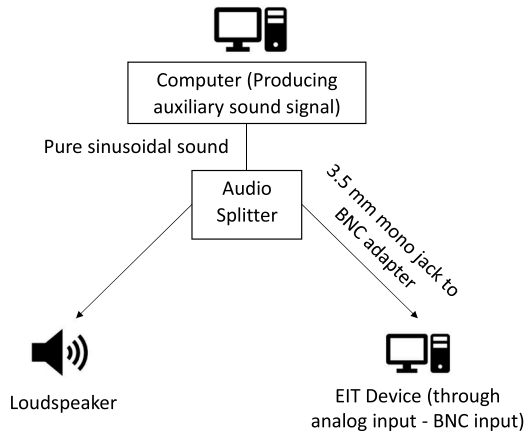
Fig. 3. Schematic representation of the synchronization system based on the use of an auxiliary device.

the Littmman Extended filter (EXTD).

2.2.2. Feature extraction

Several features have been extracted from the two sources (respiratory sound and EIT). For the sound-related features, we computed the spectrogram representation (STFT) of each audio with a 256 ms Hamming window and with 90% overlap. Then, 81 features were extracted from each frame of the spectrogram: 25 spectral features, 26 MFCC features, and 30 melodic features [64]. Several EIT features were extracted at a global and regional level from each complete EIT file. We have considered eight different regions of interest (ROIs) for feature extraction as defined in [56]. The features were extracted for each complete EIT file. Table 3 presents a brief description of each considered feature.

Both audio and EIT features were calculated using MATLAB 2022b. Most audio features were extracted using the MIR Toolbox 1.7.2 [65]. After audio and EIT feature extraction, several statistical moments (mean, median, max, min, std) were used to represent each sample (that is, features were aggregated over the whole recordings). For the impedance curve correlations features, no statistical moments were computed, as these features correspond to a single value. This resulted in a total of 405 audio features and 246 EIT features. In the supplementary material a document can be found with the name of all extracted features.

2.2.3. Classifiers

We used six shallow machine learning algorithms to classify the respiratory sound and EIT samples: linear SVM (SVMlin), SVM with radial basis function (SVMrbf), k-nearest neighbor (knn), Ensemble of bagged decision trees (treebag), decision tree (DecisionTree), and random undersampling boosting (RUSBoost). All the classifiers were trained and tested on a 5-fold cross-validation scheme. Moreover, we have also performed hyperparameter optimization of the models. Their hyperparameters were optimized on a validation set containing 10% of the training set, with a stratified division maintaining the class ratio. Bayesian optimization [66] was used to optimize the following hyperparameters of each model: box constraint and kernel scale for SVMlin and SVMrbf; distance metric, number of neighbors for knn; learning rate, number of variables to sample, number of learning cycles, minimum leaf size, and maximum number of splits for treebag and RUSBoost; and maximum number of splits and minimum leaf size for DecisionTree. After the training optimization, the models with the best hyperparameters were then applied to the independent test set. All classifiers were trained and tested in MATLAB 2022b. We also tested two filter-based feature selection methods (ReliefF and minimum redundancy maximum relevance (MRMR)), but they did not increase the classification performance of the models. Therefore, we opted not to show these results.

Apart from the six shallow machine learning models, we also developed a baseline deep learning model, namely a CNN. The architecture of the proposed model is presented in Fig. 6. Similarly to the shallow models, the CNNs were also trained and tested on the same 5-fold cross-validation scheme. The model is composed of two branches, one for EIT and another for respiratory sound. Additionally, each branch
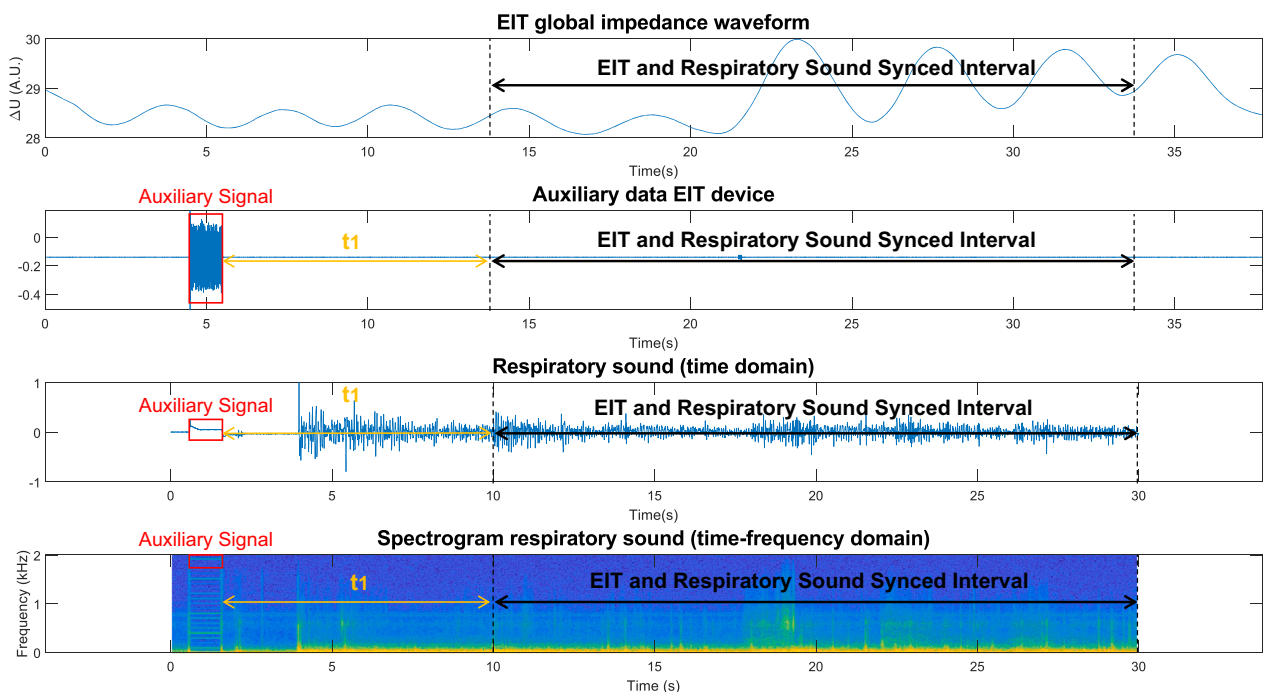

Fig. 4. Example of post-acquisition synchronization for a TbDb acquisition. (t1 - interval from the ending of the auxiliary signal until the end of the synchronization period (initial 10 seconds); **ΔZ-impedance variation; A.U.-arbitrary units**).
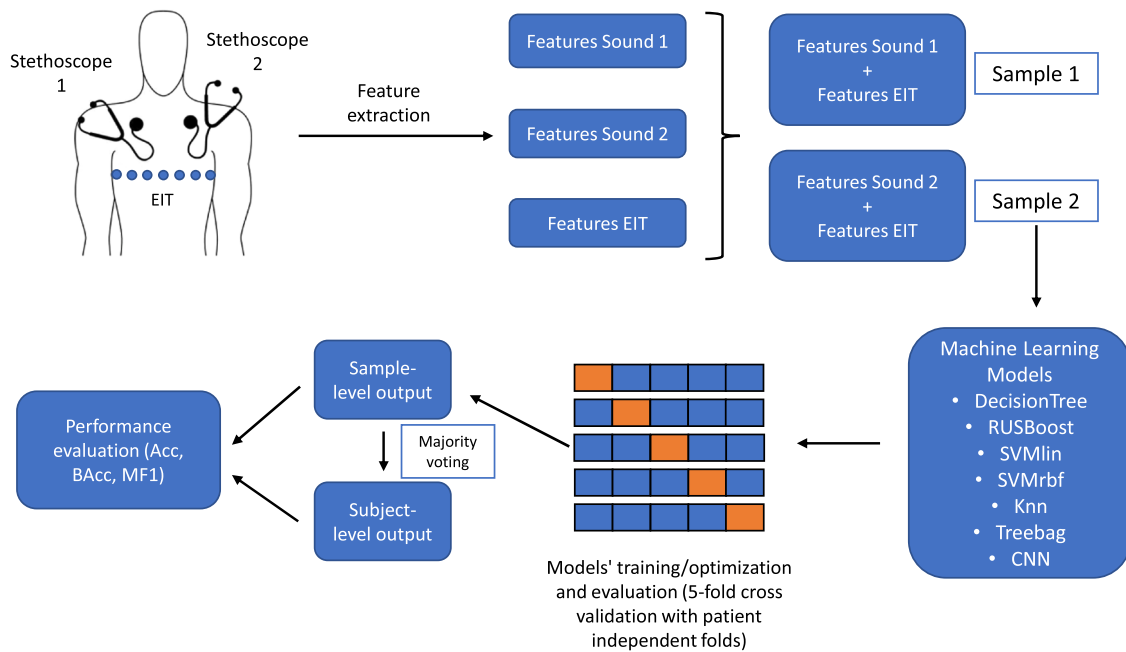
Fig. 5. Schematic representation of the automatic classification pipeline. For subjects recorded in Aveiro (single audio channel) only "Sample1" was considered. (Acc - Accuracy; BAcc - Balanced accuracy; MF1 - Macro F1).

was composed of three convolutional blocks with different filters. After the convolutional blocks, we employed a 2-dimensional global max pooling layer. Lastly, we flattened the extracted/learned features to one dimension and concatenated them when respiratory sound and EIT were combined. As the final layer, we used a dense layer with a softmax activation function to output the probability of each class. If only one input was considered, only the corresponding branch was used. Since EIT data were a temporal sequence of 2-dimensional images (bio-impedance distribution maps), the EIT branch was time distributed; that is, the convolutional operations on the EIT branch were applied to each EIT image/frame separately.

Following a similar approach to [53], we have considered only the initial five seconds of the signals as inputs for the CNN model, both for the respiratory sound and the EIT. We have computed the spectrograms (STFT) of the respiratory sound to use as input for the respiratory sound branch. To compute the STFT, a 128 ms Blackman-Harris window with 80% overlap was applied. For the Fast Fourier Transform (FFT), 512 points were used, resulting in 391-bin log-magnitude spectrograms. For the EIT branch, we used the reconstructed frames of each signal as described in Section 2.2.1 and considered only the frames corresponding to the first five seconds. The resulting input shapes for the respiratory sound and EIT branches were (257,195,1), and (165,32,32,1), respectively.

The CNN models were trained for 100 epochs with a batch size of 16. Simultaneously with the training process, the model was evaluated using the validation subset at every new epoch to save only the set of weights with the lowest validation loss. As the loss function, we used the categorical cross-entropy. Similarly to the shallow classification models, 10% of the training dataset was considered for validation. All CNN models were developed using Tensorflow v2.11.0.

2.2.4. Evaluation

The development of automated differential diagnosis methods for the detection of respiratory diseases is a valuable tool that can aid clinicians and facilitate the diagnosis of a particular subject. These methods can be particularly beneficial when considering their deployment in remote monitoring applications. Considering this, we designed several tasks for developing and assessing such methods under different scenarios. The tasks are presented below.

Evaluation tasks: We have considered six tasks, of different complexity, for classifying respiratory diseases: Tasks A1, A2, A3, B1, B2, and B3 (see Table 4). The tasks were divided into two main groups based on discriminating between different class groups at different levels (A - sample level, B - subject level) with different granularity.

Task A (Respiratory disease classification at sample level): 1)**Task A1** is a binary classification task aiming at classifying samples as *Healthy* and *Non-healthy*; 2) **Task A2** is a 3-class classification task aiming at classifying samples as *Healthy, Obstructive*, and *Restrictive*; 3) **Task A3** is a 5-class classification task aiming at classifying samples as *Healthy, COPD, Asthma, ILD, Pulmonary Infection*.

Task B (Respiratory disease classification at subject level): 1) **Task B1** is a binary classification task aiming at classifying subjects as *Healthy* and *Non-healthy*; 2) **Task B2** is a 3-class classification task aiming at classifying subjects as *Healthy, Obstructive*, and *Restrictive*; 3) **Task B3** is a 5-class classification task aiming at classifying samples as *Healthy, COPD, Asthma, ILD, Pulmonary Infection*.

Table 4 presents a summary of the different classification tasks. In tasks A2 and B2, the *Obstructive* class included the Asthma and COPD diagnoses; the *Restrictive* class included the ILD and Pulmonary Infection diagnoses.

Data split: We have separated the complete database into training and testing sets multiple times to train and evaluate the performance of the classification models. We have considered a patient-independent stratified 5-fold cross-validation strategy for splitting the data. With this strategy, every subject belonged exclusively to either the training or testing set of each fold. Moreover, we used every subject to evaluate the model since everyone was in the test set once. Typically, samples from the same patient tend to have some similarity within themselves, which might lead to overly optimistic performance results whenever data from the same subject is in both sets. Previous studies have reported this behavior [56]. Additionally, for real-world applications, the main objective is usually to deploy the models in new subjects, stressing the need for patient-independent validation. Data splits created for tasks A1, A2, and A3, were used on the corresponding B tasks. The subject separation for each task is available online together with the database.

Evaluation metrics: Given the imbalanced distribution in the number of samples of each class, we have considered the macro mean of the F1 Score (F1) and the balanced accuracy (BAcc) to evaluate the

Table 3
Brief description of the extracted features from respiratory sound and EIT.

Source		Features	Description
Sound	Spectral	Spectral Centroid	Center of mass of the spectral distribution
		Spectral Spread	Variance of the spectral distribution
		Spectral Skewness	Skewness of the spectral distribution
		Spectral Kurtosis	Excess kurtosis of the spectral distribution
		Zero-crossing Rate	Waveform sign-change rate
		Spectral Entropy	Estimation of the complexity of the spectrum
		Spectral Flatness	Estimation of the noisiness of a spectrum
		Spectral Roughness	Estimation of the sensory dissonance
		Spectral Irregularity	Estimation of the spectral peaks' variability
		Spectral Flux	Euclidean distance between the spectrum of successive frames
		Spectral Flux Inc	Spectral flux with focus on increasing energy solely
		Spectral Flux Halfwave	Halfwave rectified spectral flux
		Spectral Flux Median	Median filtered spectral flux
		Spectral Brightness	Amount of energy above 100, 200, 400, and 800 Hz
		Brightness 400 Ratio	Ratio between spectral brightness at 400 and 100 Hz
		Brightness 800 Ratio	Ratio between spectral brightness at 800 and 100 Hz
		Spectral Rolloff	Frequency such that 95, 75, 25, and 5% of the total energy is contained below it
		Rolloff Outlier Ratio	Ratio between spectral rolloff at 5 and 95%
		Rolloff Interquartile Ratio	Ratio between spectral rolloff at 25 and 75%
	MFCC	MFCC	13 Mel-frequency cepstral coefficients
		Delta-MFCC	1st-order temporal differentiation of the MFCCs
	Melodic	Pitch	Fundamental frequency estimation
		Pitch Smoothing	Moving average of the pitch curve with lengths of 100, 250, 500, and 1000 ms
		Inharmonicity	Partials non-multiple of fundamental frequency
		Inharmonicity Smoothing	Moving average of the inharmonicity curve with lengths of 100, 250, 500, and 1000 ms
		Voicing	Presence of fundamental frequency
		Voicing Smoothing	Moving average of the voicing curve with lengths of 100, 250, 500, and 1000 ms
EIT		Ventilation Ratios	Ratio between the sum of all pixel values from two certain regions
		Coefficient of Variation	Statistical measure that characterizes the relative magnitude of the standard deviation of a EIT frame with respect to its mean (quantifies the homogeneity of the volume distribution)
		Global Inhomogeneity Index	Measure that quantifies the homogeneity of the volume distribution and it is defined as the summation of the absolute difference between median value and every pixel in a specific region
		Regional Ventilation Delay	Expresses the delay between the global start of inspiration and the point in time where the regional impedance curve reaches a certain threshold (set to 40%)
		Impedance Curve Correlation	Correlation between the GIC and the regional impedance curves, and between the regional impedance curves within themselves

classification models. Moreover, we have also considered the global classification accuracy. Metrics for the multi-class classification problems were computed in a one-vs-all fashion. The mathematical expressions for each considered metric are presented below:

$$Accuracy = \frac{TP + TN}{TP + TN + FP + FN} \tag{1}$$

$$Precision = \frac{TP}{TP + FP} \tag{2}$$

$$Recall = \frac{TP}{TP + FN} \tag{3}$$

$$F1Score(F1) = \frac{2 \times Precision \times Recall}{Precision + Recall} \tag{4}$$

$$MacroF1 = \frac{F1_{Class1} + F1_{Class2} + \dots + F1_{ClassN}}{N} \tag{5}$$

$$BalancedAccuracy = \frac{Recall_{Class1} + Recall_{Class2} + \dots + Recall_{ClassN}}{N} \tag{6}$$

where TP (True Positives) are the samples of the relevant class that are correctly classified; TN (True Negatives) are the samples of the other classes that are correctly classified; FP (False Positives) are the samples that are incorrectly classified as the relevant class; FN (False Negatives) are the samples of the relevant class that are incorrectly classified. For multi-class classification, the evaluation metrics were computed in a one-vs-all fashion.

3. Results

3.1. Database demographics and structure

A total of 78 subjects from two countries (Portugal and Greece), healthy and non-healthy, were considered in the data collection for this database. All Portuguese data were recorded at the Respiratory Research and Rehabilitation Laboratory (Lab3R) of the School of Health Sciences, University of Aveiro; participants were enrolled in a 12-week community-based pulmonary rehabilitation program. Greek participants were recruited at the George Papanikolaou General Hospital of Thessaloniki (outpatient clinic and intensive care unit). Non-healthy subjects suffered from various respiratory conditions (COPD, asthma, interstitial lung disease (ILD), among others). The demographic aspects and characteristics of the database as well as the distribution of subjects per primary diagnosis, are presented in Table 5. All primary diagnoses were assigned by pulmonologists.

The audio files of the database were stored in *.wav* format, while EIT files were stored in *.eit* format. The signals from each subject were grouped in individual folders. Within each subject's folder, two folders were created, one for respiratory sound (Sound) and one for EIT (EIT). Furthermore, inside each sound folder, there were three different subdirectories, one for each filter type used to extract the recorded respiratory sounds (BELL, DIAP, EXTD). We included a tree diagram representation of the organization of the folders in the database in the
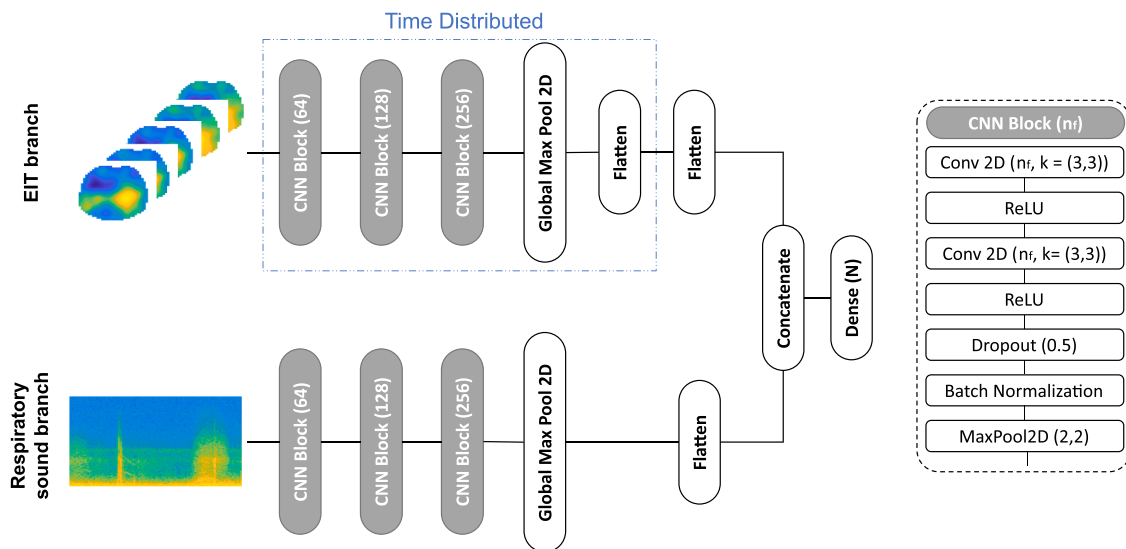
Fig. 6. Architecture of the proposed dual-input CNN baseline model. (nf - number of filters; N - number of classes according to the task; Conv2D - 2D convolution layer; ReLU - Rectified Linear Unit).

Table 4
Summary of all classification tasks with respective disease distributions.

Classification level	Task	Classes
Sample (Task A)	A1	Healthy, Non-healthy
	A2	Healthy, Obstructive, Restrictive
	A3	Healthy, COPD, Asthma, ILD, Pulmonary Infection
Subject (Task B)	B1	Healthy, Non-healthy
	B2	Healthy, Obstructive, Restrictive
	B3	Healthy, COPD, Asthma, ILD, Pulmonary Infection

supplementary material. Sound file names were structured as follows: "*SubjectID_RecordingID_AuscultationPoint.wav*". EIT file names were structured as follows: "*SubjectID_RecordingDateTime.eit*".

The database also comprises a metadata folder, where all the characteristics of each subject are available. Moreover, the data splits used for the 5-fold cross-validation evaluation scheme of the machine learning models are also available.

3.2. Respiratory diseases automatic classification results

This section presents the results obtained for the classification models in the six considered evaluation tasks. Table 6 displays the results obtained at sample-level and Table 7 at subject-level, respectively. The results for each individual class in all tasks can be found in the supplementary material.

The subject-level predictions were obtained based on the individual predictions of each sample. We took all predictions at the sample level for each subject in each test set fold and determined a final class based on a majority voting process. Thus, the class attributed to each subject was based on the most common class in its samples. In case of a draw in the voting process, we assigned the class based on a conservative approach. A subject was classified as healthy in all cases where a draw occurred. For instance, in task B1, a subject with five individual samples classified as healthy, and five non-healthy, was classified as healthy. This rationale was applied in tasks B2 and B3. It should be noted that for task B, no new models were trained. In tasks B1, B2, and B3, the models trained for tasks A1, A2, and A3, were used, respectively.

The machine learning models were trained using different feature sets based on their source. Three sets of features were considered: sound-based, EIT-based, and sound and EIT combined features. The main objective of this breakdown was to understand the individual

contribution of each data source for the differential diagnosis of respiratory diseases and whether their combination would enhance the performance of the models. The presented results were divided according to the set of features used.

In task A1, the radial basis function SVM classifier (SVMrbf), using both respiratory sound and EIT-derived features, was the best performer, with a mean balanced accuracy value of 77.9±13.1% and a mean macro F1 of 79.0±12.9%. When considering the subject-level classification, task B1, the SVMrbf model with both feature sets, is again the model that achieved the highest results, with a mean balanced accuracy value of 90.0±22.4% and a macro F1 of 89.3±23.9%.

For the 3-class classification problem at sample level, task A2, the model with the best performance was the SVMrbf using both respiratory sound and EIT-derived features, with a mean balanced accuracy value of 51.6±9.7% and a mean macro F1 of 51.7±8.7%. Likewise, after the transposition of the results for the subject level, the same model, SVMrbf with respiratory sound and EIT features, presented a higher mean balanced accuracy, 61.4±11.8%, and a mean macro F1 of 60.6±12.0%.

Lastly, in the 5-class classification problem at sample level, task A3, the model with the best performance was the RUSBoost using sound and EIT features, with a mean balanced accuracy value of 38.6±13.1% and a mean macro F1 34.2±11.9%. However, in task B3, the RUSBoost model with respiratory sound features only presented the highest mean balanced accuracy, 50.8±10.6%, and the SVMlin with both feature sets presented the highest mean macro F1, 38.5±11.3%.

We have also represented the global confusion matrices for the models with higher mean balanced accuracy in every task to better understand their performance in Fig. 7. The global confusion matrices resulted from adding every fold's confusion matrix.

4. Discussion

In this study, we built the first open-access bimodal database containing respiratory sound and EIT. The database contains 1097 respiratory sounds and 795 EIT recordings from 78 participants. Besides publicly releasing the database, we proposed several baseline machine-learning systems to classify respiratory diseases using respiratory sound and EIT. We also studied the discriminating power of each source by building models using different sets of features/inputs. These baselines will set a standard for future works on the topic using this database and allow a better comparison between them.

In general, four main insights can be derived from the analysis of the

Table 5
Demographic information of database (F - Female; M - Male; #RS - Number of respiratory sound recordings; #EIT - number of EIT recordings).

	All	Aveiro	Thessaloniki
Number of subjects	78	50	28
Gender (M/F)	53/25	35/15	18/10
Age (years)	65.2 ± 13.0	67.4 ± 8.9	61.3 ± 17.6
Height (m)	1.67 ± 0.1	1.6 ± 0.1	1.7 ± 0.1
Weight (kg)	78.5 ± 18.4	75.9 ± 17.1	83.1 ± 20.1
BMI (kg/m^2)	28.1 ± 5.2	27.8 ± 5.6	28.7 ± 4.5
Number of sound recordings	1097	490	607
Number of EIT recordings	795	490	305
Duration sound recordings (hours)	7.2	2.7	4.5
Duration EIT recordings (hours)	8.2	5.4	2.8
Number of sound recordings (TbDB/TbCS)	436/661	246/244	190/417
Number of EIT recordings (TbDB/TbCS)	342/453	246/244	96/209
Average duration of TbDB sound recordings (s)	23.1 ± 4.2	19.8 ± 1.2	27.3 ± 2.7
Average duration of TbCS sound recordings (s)	24.2 ± 4.5	19.9 ± 0.7	26.7 ± 3.7
Average duration of TbDB EIT recordings (s)	37.5 ± 6.4	40.2 ± 5.1	30.4 ± 3.3
Average duration of TbCS EIT recordings (s)	37.0 ± 10.9	38.7 ± 2.8	35.1 ± 15.6
Subjects' Primary Diagnosis (#RS/#EIT)			
Asthma	8 (94/82)	7 (70/70)	1 (24/12)
COPD	32 (384/318)	26 (252/252)	6 (132/66)
Healthy	8 (176/89)	-	8 (176/89)
ILD	24 (315/242)	17 (168/168)	7 (147/74)
Pulmonary Infection	6 (128/64)	-	6 (128/64)

obtained results on the classification of respiratory diseases based on our database:

- The results in the binary classification tasks were significantly better compared to the multi-class classification problems
- Generally, the combination of sources (respiratory sound and EIT) improved the classification performance of most models

- The subject-level results were significantly better than sample-level ones in all classification tasks, highlighting the usefulness of recording multiple auscultation points
- For several of the considered metrics, the standard deviations were high

While the number of classes in the multi-class classification tasks is not very high, those are substantially more complex compared to the binary problem, particularly the discrimination between all individual diagnoses. This can be observed in the confusion matrices presented in Fig. 7, where there was a significant misclassification rate both at sample and subject levels for multi-class tasks (Fig. 7(c), Fig. 7(d), Fig. 7(e), and Fig. 7(f)). Moreover, given the unbalanced nature of the database, the models are biased towards the majority classes, which also makes the classification tasks more difficult. This behavior can also be observed in the confusion matrices presented in Fig. 7.

Another main insight derived from the analysis of the results was that the combination of respiratory sound and EIT features improved the classification performance in most cases. In fact, with the exception of task B3, the best models with regards to mean BAcc and mean macro F1 were all trained with features from both sources. For the shallow machine learning models, the feature fusion approach yielded better results for three models in tasks A1, A3, B1, B2, and B3, and four in task A2. Therefore, combining both data sources improved the performance of the models in all tasks in at least 50% of the cases for shallow models. Such results highlighted the benefits of a bimodal approach for the specific problem of respiratory disease classification. As for deep learning models (CNN), we observed that the combination of the two inputs was only beneficial in tasks A1 and B1. On the remaining tasks, the models performed generally better using only respiratory sound or EIT.

After grouping the sample predictions to obtain subject-level results, the mean balanced accuracy in the shallow models increased, on average, by approximately 3% from task A1 to B1, 6% from task A2 to B2, and 6% from task A3 to B3. Also, in task B3, the task with more classes, we observed that the model with the highest BAcc was the RUSBoost with only sound features. Such results stressed the importance of analyzing the respiratory sounds at multiple auscultation points. Moreover, multiple auscultation points can also detect a localized lesion. For instance, if the left lung is collapsed, there will be either decreased or absent respiratory sounds in that area during auscultation. Thereby, multiple auscultation points will provide a broader characterization of

Table 6
Classification results at sample level. The highest values for each metric in every task were highlighted in bold.

Source	Classifier	Task A1			Task A2			Task A3		
		Accuracy	BAcc	MacroF1	Accuracy	BAcc	MacroF1	Accuracy	BAcc	MacroF1
Sound	DecisionTree	78.7±1.8	52.8±4.3	50.5±5.7	41.9±4.0	35.7±4.5	33.3±5.3	35.7±5.2	29.2±6.9	28.0±5.7
	RUSBoost	82.5±5.2	73.2±8.6	69.9±7.9	49.9±1.7	49.2±4.9	44.9±3.2	31.5±3.2	36.3±2.1	30.5±4.3
	SVMlin	85.1±4.8	65.7±7.9	67.0±9.4	44.3±5.3	41.3±6.7	39.0±10.6	35.9±4.5	30.7±4.6	28.9±4.9
	SVMrbf	87.0±5.1	70.1±8.7	71.9±9.2	45.9±3.6	44.4±4.8	43.8±5.2	38.4±4.6	33.3±4.7	32.1±4.9
	knn	79.9±8.0	63.3±4.9	62.9±5.4	44.9±2.5	40.9±3.2	40.2±3.6	36.0±6.3	29.0±4.8	27.1±3.5
	treebag	85.4±3.6	64.2±7.6	65.4±9.3	47.0±5.4	39.1±4.0	36.3±5.4	38.8±4.0	28.4±4.4	26.6±6.7
	CNN	57.0±24.0	57.0±5.4	45.7±16.0	33.6±9.7	34.3±2.4	21.7±5.2	25.5±4.2	24.8±4.4	18.3±4.6
EIT	DecisionTree	85.7±4.0	63.8±7.1	62.3±3.1	48.4±10.3	38.0±11.0	36.4±11.6	37.0±6.9	26.0±6.3	24.5±6.6
	RUSBoost	86.8±5.9	64.4±16.0	62.4±14.5	50.2±9.0	48.7±12.1	45.6±9.3	33.8±7.9	34.1±12.0	29.1±8.8
	SVMlin	87.6±5.5	59.6±7.4	61.2±8.6	47.4±4.2	45.1±8.9	42.9±6.9	33.9±7.8	27.5±4.5	25.5±3.5
	SVMrbf	87.3±3.4	61.1±12.8	58.8±7.8	47.8±4.1	40.9±4.8	40.9±6.0	33.5±5.2	25.4±4.1	23.9±3.2
	knn	86.7±4.2	55.5±11.9	54.1±11.8	51.9±5.2	46.4±6.9	44.6±5.9	37.1±8.3	29.3±7.9	26.8±6.3
	treebag	86.2±7.4	63.0±17.9	61.0±16.6	**54.0±6.3**	46.6±3.9	46.7±4.2	**42.3±9.7**	29.5±9.1	27.4±10.6
	CNN	81.5±5.2	58.5±9.6	55.4±6.2	51.3±4.1	42.6±3.3	40.7±4.1	24.6±3.4	18.8±3.5	18.3±2.7
Sound + EIT	DecisionTree	82.5±5.7	67.0±10.7	65.7±9.2	48.4±6.3	45.0±9.9	42.8±11.0	35.0±7.3	28.8±6.6	27.1±5.4
	RUSBoost	83.7±6.4	61.9±10.0	62.1±11.4	49.8±8.9	46.7±12.0	46.7±12.3	38.4±10.5	**38.6±13.1**	**34.2±11.9**
	SVMlin	86.6±3.0	73.9±8.7	73.2±6.0	49.3±6.2	50.9±8.5	50.4±8.7	39.2±9.8	34.2±9.0	31.3±8.5
	SVMrbf	**89.9±6.4**	**77.9±13.1**	**79.0±12.9**	49.4±6.8	**51.6±9.7**	**51.7±8.7**	37.5±8.0	32.5±7.7	29.8±6.7
	knn	76.8±4.8	58.9±5.5	57.9±5.4	47.8±5.9	45.1±4.8	43.5±4.4	30.4±4.0	27.0±4.0	24.5±3.1
	treebag	85.6±7.8	63.5±13.9	64.3±17.2	48.4±9.4	43.9±11.1	44.0±13.9	41.6±8.0	32.4±7.4	29.1±7.6
	CNN	78.4±9.1	59.7±11.0	60.1±13.0	35.0±14.6	34.6±8.2	27.7±12.0	19.1±8.1	19.8±6.2	15.9±4.9

Table 7

Classification results at subject level. The highest values for each metric in every task were highlighted in bold.

Source	Classifier	Task B1			Task B2			Task B3		
		Accuracy	BAcc	MacroF1	Accuracy	BAcc	MacroF1	Accuracy	BAcc	MacroF1
Sound	DecisionTree	88.6±5.0	49.3±1.6	46.9±1.4	50.1±5.9	37.8±5.0	34.5±7.9	52.8±13.5	38.7±20.0	32.8±17.7
	RUSBoost	93.8±8.8	87.9±23.4	84.9±24.1	57.8±6.8	61.4±12.0	51.5±10.1	37.4±9.5	**50.8±10.6**	37.4±13.2
	SVMlin	91.1±3.3	55.0±11.2	54.3±15.3	51.4±5.9	50.8±15.3	46.8±18.7	46.4±10.0	38.5±6.0	35.5±7.2
	SVMrbf	92.4±5.2	65.0±22.4	64.6±24.8	57.7±3.6	58.6±11.2	53.5±12.0	48.8±6.6	38.6±5.1	34.9±6.5
	knn	92.3±2.7	68.6±18.5	67.9±17.9	52.6±2.6	48.3±14.3	42.6±15.1	46.2±8.2	36.5±15.1	30.5±14.2
	treebag	91.1±3.3	55.0±11.2	54.3±15.3	53.8±9.8	37.8±8.6	34.9±8.3	43.8±6.7	26.9±7.4	21.9±9.4
	CNN	60.7±36.0	51.4±2.9	34.6±16.0	36.3±19.5	33.3±0.0	16.9±7.8	23.1±8.5	24.6±10.0	14.1±7.0
EIT	DecisionTree	91.1±5.7	77.9±19.6	74.2±19.3	55.5±17.4	45.0±19.7	43.0±20.2	43.5±14.0	24.8±8.7	22.6±7.5
	RUSBoost	90.0±9.5	68.6±28.7	67.3±29.9	52.7±12.3	50.6±18.1	42.8±13.8	42.5±16.2	41.2±18.3	38.1±17.8
	SVMlin	89.8±3.2	50.0±0.0	47.3±0.9	51.6±11.8	51.7±20.1	48.2±19.5	38.6±10.7	30.6±7.8	27.3±4.0
	SVMrbf	89.8±3.2	59.3±20.8	54.0±15.4	47.4±7.0	38.3±10.0	38.1±13.8	41.1±9.7	30.6±8.6	28.0±6.2
	knn	91.2±5.5	60.0±22.4	57.7±23.7	52.7±14.5	49.7±20.3	45.2±22.4	43.8±11.3	34.3±13.9	29.0±11.7
	treebag	91.3±8.4	69.3±28.1	67.6±29.6	**61.7±9.4**	53.6±11.0	52.3±11.9	51.6±11.8	34.5±13.9	30.9±14.3
	CNN	88.5±2.4	67.1±22.5	60.1±16.6	57.5±6.5	44.2±4.8	39.7±6.0	23.1±5.0	13.5±2.5	13.4±2.0
Sound + EIT	DecisionTree	88.5±5.2	72.1±23.3	65.1±18.2	57.8±10.7	55.3±20.5	52.6±19.9	44.7±14.0	33.2±15.3	29.0±13.7
	RUSBoost	89.9±7.1	68.6±27.1	63.9±25.3	59.3±11.3	53.9±21.3	50.3±20.8	45.1±14.8	43.1±18.5	37.5±17.2
	SVMlin	96.3±5.6	85.0±22.4	85.7±23.2	56.4±5.0	60.3±7.1	59.2±7.1	50.1±11.6	43.0±12.4	**38.5±11.3**
	SVMrbf	**97.5±5.6**	**90.0±22.4**	**89.3±23.9**	53.8±10.3	**61.4±11.8**	**60.6±12.0**	48.8±8.1	39.0±6.3	34.7±5.0
	knn	87.2±4.4	52.9±12.5	53.2±15.9	59.2±8.7	48.6±16.7	45.2±18.2	35.8±10.7	30.2±14.8	25.4±13.9
	treebag	91.3±8.4	69.3±28.1	67.6±29.6	56.6±9.7	45.0±19.2	42.4±20.8	**53.9±7.6**	36.5±7.9	30.8±7.1
	CNN	87.1±7.4	57.1±13.0	58.1±15.0	39.4±16.5	37.2±3.4	23.9±10.7	15.7.0±16.0	17.6±13.0	10.0±10.0

the general health of a subject's respiratory system.

From the analysis of the results in Table 6 and Table 7, we also observed that, for some of the considered metrics, the standard deviation values were high. Those were mainly related to our approach to training and testing our models. Since we used 5-fold stratified cross-validation with subject-independent folds, the number of subjects in the test set for the minority classes was relatively small. Notwithstanding, using this evaluation approach provides a better assessment of the performance of the models than just considering a hold-out validation with a single data split, which was the approach used for most databases previously published in the literature listed in Table 1. Moreover, if, in a specific fold, the models performed poorly in one of the minority classes, that would have introduced a high variation in the evaluation metrics, both at the sample and subject level. This was specially the case at the subject-level classification tasks (tasks B1, B2, and B3), where the deviations were higher. Lastly, since every patient was used in the test, there might have been some more complex folds than others. Considering that there is an inherent difference/heterogeneity between samples of different subjects, this could have also introduced a higher variability in the results.

Automatic classification of respiratory diseases is a complex task, as demonstrated by establishing this database. Despite the good results published in the literature for this specific task using solely respiratory sounds, there are still several areas for improvement before deploying such methods in real digital health-driven applications, namely the explainability and interpretability of the models. With the use of respiratory sound and EIT, we can complement the findings of each source to have a higher degree of confidence in the developed models. Moreover, there is also the need for more extensively validated models with different databases obtained under different conditions. This is a crucial step to assess the robustness of the developed models and their generalization capability.

Despite the problem of automatically diagnosing respiratory diseases based on the respiratory sound being a common problem in the literature [25], the same cannot be said about EIT. With regards to EIT, few studies leveraged its use for classification purposes. However, as demonstrated in this study, machine learning models trained on EIT features/data can obtain results comparable to those obtained with respiratory sounds for the automated classification of respiratory diseases.

By using this database, future works can target the development of automated methods for diagnosing respiratory diseases using a bimodal approach, which can yield better results. Moreover, they might also solely focus on EIT for that same purpose, as the imaging modality is vastly unexplored in this context. Future works might also study other data-driven techniques, such as other deep learning architectures or ensemble methodologies, to combine respiratory sound and EIT. For instance, the two data sources might be combined at lower or higher levels (signal-level or decision-level fusion, respectively)[61]. Another possible area for improvement of the classification performance is the development of preprocessing techniques. Data augmentation techniques, both at the data and algorithm level, can also be employed to address the data imbalance issue. For instance, generative adversarial networks or variational autoencoders might be used to artificially generate new samples and increase the performance of the classification models [49,67]. Such approaches will particularly help to increase the performance of deep-learning models as these tend to scale better as the number of available samples increases.

Apart from being used to develop algorithms for the automated diagnosis of respiratory diseases, the database can also be used for other tasks, leveraging the complementary information provided by the respiratory sounds and EIT. As pointed out in [68], there is great potential for the integration of EIT with other bio-signals. For instance, EIT can identify a less ventilated area of the chest (e.g., left lung), and lung sound algorithms might target the auscultation points related to that area to derive further insights. Therefore, future works using this database might only target specific auscultation points and develop more targeted solutions. Besides this approach, specific solutions might also be developed by studying differences in the characteristics of respiratory sound and EIT in the different protocol stages. Such differences might convey relevant information for the differential diagnosis. For instance, this analysis might be relevant when comparing EIT-derived metrics extracted during tidal and deep breathing, as the asymmetry in the bioimpedance distribution in the lungs might be emphasized during deep breathing.

Another use case can be the complete characterization of respiratory sounds. With respiratory sounds, we can detect the presence of adventitious sounds (usually present in the case of respiratory disorder). On the other hand, with the synchronous EIT signal, we can detect the respiratory phase where those occur. The timing of the adventitious sounds with the respiratory cycle is of great clinical relevance [69]. Currently, we still do not have individual annotations of each adventitious respiratory sound in the sound recordings. However, we intend to release them in a future database update with the respective time stamps
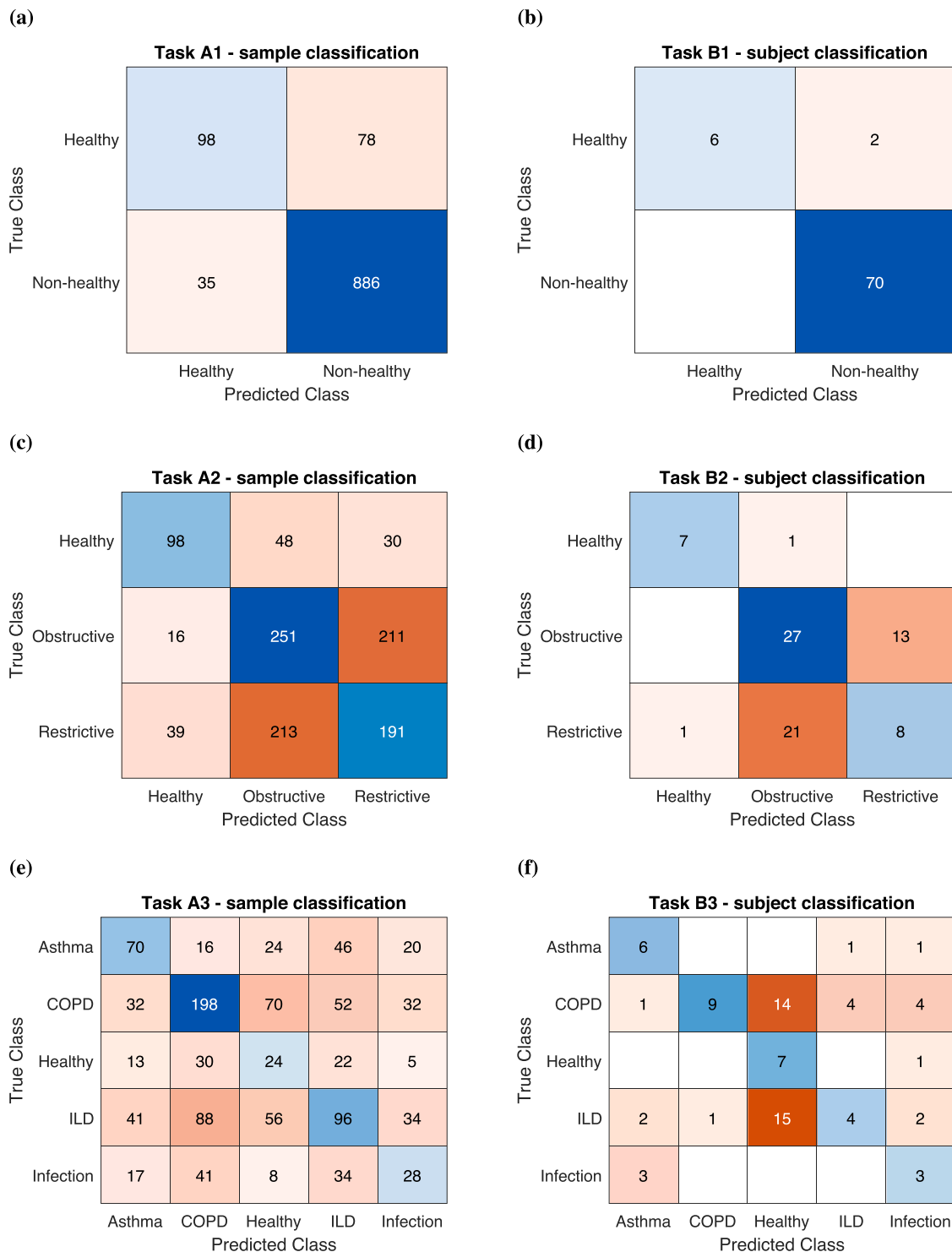
(a)

(b)

(c)

(d)

(e)

(f)

Fig. 7. Confusion matrices of the best models in all four tasks (each confusion matrix was obtained by adding the confusion matrices of all folds in the according task). a) task A1: SVMrbf - sound + EIT; b) task B1: SVMrbf - sound + EIT; c) task A2: SVMrbf - sound + EIT; d) task B2: SVMrbf - sound + EIT; e) task A3: RUSBoost - sound + EIT; d) task B3: RUSBoost - sound.

of the adventitious sounds.

Besides the complementary information provided by respiratory sound and EIT, the database can also be used to take advantage the complementary information provided by the multi-channel sound recordings. As pointed in [54], spatial information obtained through several acquisition channels can improve the robustness of the developed methods and provide and offer supplementary insights.

Some of the limitations of this database are related to differences

between healthy and non-healthy subjects. Healthy subjects were from a significantly younger age group than subjects with respiratory conditions. Besides, the database presents a significantly uneven subject distribution for the different diseases/classes. Also, the proposed solution to synchronize the respiratory sound and EIT is subject to error, which we could not estimate quantitatively. The error is mainly related to human error associated with manually identifying the auxiliary signal in both data sources. Lastly, even though the multi-channel recordings

were gathered simultaneously, they are not synchronous as they were collected using two independent devices without any external trigger to allow for post-acquisition alignment.

In the future, we aim to collect further data and gather long-term recordings so that methods to monitor the evolution of patients over time can be developed. Moreover, we also aim to integrate synchronous respiratory sound and EIT data collected with a wearable device developed under the scope of the WELMO project and integrate them into the current database [12,18,70].

5. Conclusion

With this work, we aim to further stimulate the development of automated methodologies to monitor and assess respiratory function, particularly using EIT. We believe there are significant gains to be obtained in the evolving field of digital health/medicine by merging the information from respiratory sounds and EIT, as these two sources map different aspects of the function of the respiratory system and can provide complementary information. Ultimately, we hope this database can serve as a foundation for researchers to build new algorithms and further propel the automated monitoring of respiratory function, aiming to improve the quality of life of patients suffering from such diseases. Moreover, this database can further aid the development of new wearable systems capable of recording multiple data sources.

Besides publicly releasing the database, we proposed several baseline machine-learning systems to classify respiratory diseases using respiratory sound and EIT. We also studied the discriminating power of each source by building models using different sets of features/inputs. These baselines will set a standard for future works on the topic using this database and allow a better comparison between them.

Ethical approval

The data collection for the current study was approved by two independent ethic committees approved in each country where the acquisitions took place: an approval was granted by the Nursing School of Coimbra (ESEnfC) in Portugal (Reference AD1 P721-10/2020) and by the Scientific Council of General Papanikolaou Hospital in Greece (Reference 51st/252/4-3-2021). We have complied with all relevant ethical regulations. Informed written consent was obtained from all participants before examinations.

Declaration of Competing Interest

The authors declare no competing interests.

Data availability

The database is available at https://data.mendeley.com/datasets/f43c7snks5/1 and https://github.com/DiogoMPessoa/BRACETS-Bimodal-Repository-of-Auscultation-Coupled-with-Electrical-Impedance-Thoracic-Signals. To have access to the original audio files from Aveiro with the synchronization period (initial 10 seconds), contact the authors.

Acknowledgments

Supplementary material

Supplementary material associated with this article can be found, in the online version, at doi:10.1016/j.cmpb.2023.107720

References

[1] G.J. Gibson, R. Loddenkemper, B. Lundbäck, Y. Sibille, Respiratory health and disease in Europe: the new European lung white book, European Respiratory Journal 42 (3) (2013) 559–563, https://doi.org/10.1183/09031936.00105513.

[2] World Health Organization (WHO), The top 10 causes of death, 2023, https://www.who.int/news-room/fact-sheets/detail/the-top-10-causes-of-death.

[3] GOLD, 2023 GOLD reports - global initiative for chronic obstructive lung disease - GOLD, 2023, [Accessed 02-Feb-2023], https://goldcopd.org/2023-gold-report-2/.

[4] S. Fouzas, M.B. Anthracopoulos, A. Bohadana, Clinical Usefulness of Breath Sounds, Springer International Publishing, Cham, 2018, pp. 33–52.

[5] D. Hayes, S. Kraman, The physiologic basis of spirometry, Respir Care 54 (2009) 1717–1726.

[6] M. Sarkar, I. Madabhavi, N. Niranjan, M. Dogra, Auscultation of the respiratory system, Ann Thorac Med 10 (3) (2015) 158, https://doi.org/10.4103/1817-1737.160831.

[7] Y. Kim, Y. Hyon, S. Lee, S.-D. Woo, T. Ha, C. Chung, The coming era of a new auscultation system for analyzing respiratory sounds, BMC Pulm Med 22 (1) (2022), https://doi.org/10.1186/s12890-022-01896-1.

[8] M.R. Miller, J. Hankinson, V. Brusasco, F. Burgos, R. Casaburi, A. Coates, R. Crapo, P. Enright, C.P.M. van der Grinten, P. Gustafsson, R. Jensen, D.C. Johnson, N. MacIntyre, R. McKay, D. Navajas, O.F. Pedersen, R. Pellegrino, G. Viegi, J. Wanger, Standardisation of spirometry, European Respiratory Journal 26 (2) (2005) 319–338, https://doi.org/10.1183/09031936.05.00034805.https://erj.ersjournals.com/content/26/2/319.full.pdf

[9] A. Marques, A. Oliveira, C. Jácome, Computerized adventitious respiratory sounds as outcome measures for respiratory therapy: a systematic review, Respir Care 59 (5) (2014) 765–776, https://doi.org/10.4187/respcare.02765.https://rc.rcjournal.com/content/59/5/765.full.pdf

[10] S. Reichert, R. Gass, C. Brandt, E. André, Analysis of respiratory sounds: state of the art, Clin Med Circ Respirat Pulm Med 2 (2008) CCRPM.S530, https://doi.org/10.4137/CCRPM.S530.PMID: 21157521

[11] V. Kilintzis, N. Beredimas, E. Kaimakamis, L. Stefanopoulos, E. Chatzis, E. Jahaj, M. Bitzani, A. Kotanidou, A.K. Katsaggelos, N. Maglaveras, Cocross: an ICT platform enabling monitoring recording and fusion of clinical information chest sounds and imaging of covid-19 ICU patients, Healthcare 10 (2) (2022), https://doi.org/10.3390/healthcare10020276.https://www.mdpi.com/2227-9032/10/2/276

[12] G. Yilmaz, M. Rapin, D. Pessoa, B.M. Rocha, A.M. de Sousa, R. Rusconi, P. Carvalho, J. Wacker, R.P. Paiva, O. Chételat, A wearable stethoscope for long-term ambulatory respiratory health monitoring, Sensors 20 (18) (2020), https://doi.org/10.3390/s20185124.https://www.mdpi.com/1424-8220/20/18/5124

[13] A.R. Watson, R. Wah, R. Thamman, The value of remote monitoring for the covid-19 pandemic, Telemedicine and e-Health 26 (9) (2020) 1110–1112, https://doi.org/10.1089/tmj.2020.0134.PMID: 32384251

[14] I. Frerichs, Electrical impedance tomography (EIT) in applications related to lung and ventilation: a review of experimental and clinical activities, Physiol Meas 21 (2) (2000) R1, https://doi.org/10.1088/0967-3334/21/2/201.

[15] W.R. Hendee, New imaging techniques. Oncologic Imaging, Elsevier, 2002, pp. 39–54, https://doi.org/10.1016/b0-72-167494-1/50006-2.

[16] S. Egan, G.P. Curley, What is the role of PEEP and recruitment maneuvers in ARDS?. Evidence-Based Practice of Critical Care Elsevier, 2020, pp. 50–56.e1, https://doi.org/10.1016/b978-0-323-64068-8.00017-1.

[17] I. Frerichs, M.B.P. Amato, A.H. van Kaam, D.G. Tingay, Z. Zhao, B. Grychtol, M. Bodenstein, H. Gagnon, S.H. Böhm, E. Teschner, O. Stenqvist, T. Mauri, V. Torsani, L. Camporota, A. Schibler, G.K. Wolf, D. Gommers, S. Leonhardt, A. A. and, Chest electrical impedance tomography examination, data analysis, terminology, clinical use and recommendations: consensus statement of the TRanslational EIT developmeNt stuDy group, Thorax 72 (1) (2016) 83–93, https://doi.org/10.1136/thoraxjnl-2016-208357.

[18] I. Frerichs, R. Paradiso, V. Kilintzis, B.M. Rocha, F. Braun, M. Rapin, L. Caldani, N. Beredimas, R. Trechlis, S. Suursalu, C. Strodthoff, D. Pessoa, O. Chételat, R. P. Paiva, P. de Carvalho, N. Maglaveras, N. Weiler, J. Wacker, Wearable pulmonary monitoring system with integrated functional lung imaging and chest sound recording: a clinical investigation in healthy subjects, Physiol Meas 44 (4) (2023) 045002, https://doi.org/10.1088/1361-6579/acc82a.

[19] I. Frerichs, B. Vogt, J. Wacker, R. Paradiso, F. Braun, M. Rapin, L. Caldani, O. Chételat, N. Weiler, Multimodal remote chest monitoring system with wearable sensors: a validation study in healthy subjects, Physiol Meas 41 (1) (2020) 015006, https://doi.org/10.1088/1361-6579/ab668f.

[20] S. Hong, J. Lee, H.-J. Yoo, Wearable lung-health monitoring system with electrical impedance tomography. 2015 37th Annual International Conference of the IEEE Engineering in Medicine and Biology Society (EMBC), 2015, pp. 1707–1710, https://doi.org/10.1109/EMBC.2015.7318706.

[21] C.-L. Hu, I.-C. Cheng, C.-H. Huang, Y.-T. Liao, W.-C. Lin, K.-J. Tsai, C.-H. Chi, C.-W. Chen, C.-H. Wu, I.-T. Lin, C.-J. Li, C.-W. Lin, Dry wearable textile electrodes for portable electrical impedance tomography, Sensors 21 (20) (2021), https://doi.org/10.3390/s21206789.

[22] J.-J. Huang, Y.-H. Hung, J.-J. Wang, B.-S. Lin, Design of wearable and wireless electrical impedance tomography system, Measurement 78 (2016) 9–17, https://doi.org/10.1016/j.measurement.2015.09.031.https://science/article/pii/S0263224115004984

[23] M. Rapin, F. Braun, A. Adler, J. Wacker, I. Frerichs, B. Vogt, O. Chételat, Wearable sensors for frequency-multiplexed EIT and multilead ECG data acquisition, IEEE Trans. Biomed. Eng. 66 (3) (2019) 810–820, https://doi.org/10.1109/TBME.2018.2857199.

[24] Y. Wu, D. Jiang, A. Bardill, S. de Gelidi, R. Bayford, A. Demosthenous, A high frame rate wearable EIT system using active electrode asics for lung respiration and heart rate monitoring, IEEE Trans. Circuits Syst. I Regul. Pap. 65 (11) (2018) 3810–3820, https://doi.org/10.1109/TCSI.2018.2858148.

[25] D. Pessoa, B. Machado Rocha, P. de Carvalho, R.P. Paiva, Chapter 5 - Automated respiratory sound analysis, in: R.P. Paiva, P. de Carvalho, V. Kilintzis (Eds.), Wearable Sensing and Intelligent Data Analysis for Respiratory Management, Academic Press, 2022, pp. 123–168, https://doi.org/10.1016/B978-0-12-823447-1.00003-8.https://www.sciencedirect.com/science/article/pii/B9780128234471000038

[26] R.X.A. Pramono, S. Bowyer, E. Rodriguez-Villegas, Automatic adventitious respiratory sound analysis: asystematic review, PLoS ONE 12 (5) (2017) 1–43, https://doi.org/10.1371/journal.pone.0177926.

[27] G. Druger, The chest, its signs and sounds: The examination and interpretation of physical findings of the chest : A new teaching program, Humetrics Corp, 1973.

[28] S. Lehrer, Understanding Lung Sounds: 2nd Edition, Saunders, Philadelphia, 1993.

[29] S. Lehrer, Understanding Lung Sounds: Third Edition, W.B. Saunders, Philadelphia, Pa, 2002.

[30] M. Tilkian Ara;Conover, Understanding Heart Sounds and Murmurs : With an Introduction to Lung Sounds, W.B. Saunders, Philadelphia, 2001.

[31] D. Owens, R.A.L.E. Lung Sounds 3.0, CIN: Computers, Informatics, Nursing 5 (3) (2002) 9–10.

[32] East Tennessee State University, Pulmonary Breath Sounds, http://faculty.etsu.edu/arnall/www/public_html/heartlung/breathsounds/contents.html.

[33] J.L.B. Wilkins Robert;Hodgkin, Fundamentals of Lung and Heart Sounds, Mosby, St. Louis, 2004.

[34] L.W. Wilkins, Auscultation skills : breath & heart sounds, Wolters Kluwer/Lippincott Williams & Wilkins Health, Philadelphia, 2009.

[35] D. Wrigley, Heart and Lung Sounds Reference Library, 2002.

[36] S. Kraman, Lung sounds: an introduction to the interpretation of auscultatory findings, MedEdPORTAL 3 (1) (2007) mep_2374–8265.129, https://doi.org/10.15766/mep_2374-8265.129.

[37] S. Mangione, Secrets Heart & Lung Sounds Audio Workshop 2nd Edition + Student Consult Online Access Companion to Physical Diagnosis Secrets, Elsevier, City, 2015.

[38] SoundCloud, SoundCloud Lung sounds Repository, https://soundcloud.com/search?q=lung%20sounds.

[39] B.M. Rocha, D. Filos, L. Mendes, G. Serbes, S. Ulukaya, Y.P. Kahya, N. Jakovljevic, T.L. Turukalo, I.M. Vogiatzis, E. Perantoni, E. Kaimakamis, P. Natsiavas, A. Oliveira, C. Jácome, A. Marques, N. Maglaveras, R. Pedro Paiva, I. Chouvarda, P. De Carvalho, An open access database for the evaluation of respiratory sound classification algorithms, Physiol. Meas. 40 (3) (2019), https://doi.org/10.1088/1361-6579/ab03ea.

[40] B.M. Rocha, D. Filos, L. Mendes, I. Vogiatzis, E. Perantoni, E. Kaimakamis, P. Natsiavas, A. Oliveira, C. Jácome, A. Marques, R.P. Paiva, I. Chouvarda, P. Carvalho, N. Maglaveras, A respiratory sound database for the development of automated classification, in: N. Maglaveras, I. Chouvarda, P. de Carvalho (Eds.), Precision Medicine Powered by pHealth and Connected Health, Springer Singapore, Singapore, 2018, pp. 33–37.

[41] G. Altan, Y. Kutlu, Y. Garbi, A. Özhan Pekmezci, S. Nural, Multimedia respiratory database (RespiratoryDatabase@TR): auscultation sounds and chest x-rays, Natural and Engineering Sciences 2 (3) (2017) 59–72, https://doi.org/10.28978/nesciences.349282.

[42] M. Fraiwan, L. Fraiwan, B. Khassawneh, A. Ibnian, A dataset of lung sounds recorded from the chest wall using an electronic stethoscope, Data Brief 35 (2021) 106913, https://doi.org/10.1016/j.dib.2021.106913.https://www.sciencedirect.com/science/article/pii/S2352340921001979

[43] F.-S. Hsu, S.-R. Huang, C.-W. Huang, C.-J. Huang, Y.-R. Cheng, C.-C. Chen, J. Hsiao, C.-W. Chen, L.-C. Chen, Y.-C. Lai, B.-F. Hsu, N.-J. Lin, W.-L. Tsai, Y.-L. Wu, T.-L. Tseng, C.-T. Tseng, Y.-T. Chen, F. Lai, Benchmarking of eight recurrent neural network variants for breath phase and adventitious sound detection on a self-developed open-access lung sound database-hf_lung_v1, 2021b, 2102.03049.

[44] F.-S. Hsu, S.-R. Huang, C.-W. Huang, Y.-R. Cheng, C.-C. Chen, J. Hsiao, C.-W. Chen, F. Lai, A progressively expanded database for automated lung sound analysis: an update, Applied Sciences 12 (15) (2022), https://doi.org/10.3390/app12157623.https://www.mdpi.com/2076-3417/12/15/7623

[45] F. Hsu, S. Huang, C. Su, C. Huang, Y. Cheng, C. Chen, C. Wu, C. Chen, Y. Lai, T. Cheng, N. Lin, W. Tsai, C. Lu, C. Chen, F. Lai, Improved breath phase and

[46] Q. Zhang, J. Zhang, J. Yuan, H. Huang, Y. Zhang, B. Zhang, G. Lv, S. Lin, N. Wang, X. Liu, M. Tang, Y. Wang, H. Ma, L. Liu, S. Yuan, H. Zhou, J. Zhao, Y. Li, Y. Yin, L. Zhao, G. Wang, Y. Lian, SPRSound: open-source SJTU paediatric respiratory sound database, IEEE Trans Biomed Circuits Syst (2022) 1–16, https://doi.org/10.1109/TBCAS.2022.3204910.

[47] M. Aykanat, Ö. Kiliç, B. Kurt, S. Saryal, Classification of lung sounds using convolutional neural networks, EURASIP J Image Video Process 2017 (1) (2017) 65, https://doi.org/10.1186/s13640-017-0213-2.https://www.jivp-eurasipjournals.springeropen.com/articles/10.1186/s13640-017-0213-2

[48] D. Perna, A. Tagarelli, Deep Auscultation: Predicting Respiratory Anomalies and Diseases via Recurrent Neural Networks. 2019 IEEE 32nd Int. Symp. Comput. Med. Syst. volume 2019-June, IEEE, 2019, pp. 50–55, https://doi.org/10.1109/CBMS.2019.00020.https://ieeexplore.ieee.org/document/8787435/

[49] M.T. García-Ordás, J.A. Benítez-Andrades, I. García-Rodríguez, C. Benavides, H. Alaiz-Moretón, Detecting respiratory pathologies using convolutional neural networks and variational autoencoders for unbalancing data, Sensors (Switzerland) 20 (4) (2020), https://doi.org/10.3390/s20041214.

[50] S.B. Shuvo, S.N. Ali, S.I. Swapnil, T. Hasan, M.I.H. Bhuiyan, A lightweight CNN model for detecting respiratory diseases from lung auscultation sounds using EMD-CWT-based hybrid scalogram, IEEE J Biomed Health Inform 25 (7) (2021) 2595–2603, https://doi.org/10.1109/JBHI.2020.3048006.

[51] J. Torre-Cruz, F. Canadas-Quesada, S. García-Galán, N. Ruiz-Reyes, P. Vera-Candeas, J. Carabias-Orti, A constrained tonal semi-supervised non-negative matrix factorization to classify presence/absence of wheezing in respiratory sounds, Applied Acoustics 161 (2020) 107188, https://doi.org/10.1016/j.apacoust.2019.107188.https://www.sciencedirect.com/science/article/pii/S0003682X19308540

[52] L. Fraiwan, O. Hassanin, M. Fraiwan, B. Khassawneh, A.M. Ibnian, M. Alkhodari, Automatic identification of respiratory diseases from stethoscopic lung sound signals using ensemble classifiers, Biocybernetics and Biomedical Engineering 41 (1) (2021) 1–14, https://doi.org/10.1016/j.bbe.2020.11.003.

[53] M. Fraiwan, L. Fraiwan, M. Alkhodari, O. Hassanin, Recognition of pulmonary diseases from lung sounds using convolutional neural networks and long short-term memory, J Ambient Intell Humaniz Comput 13 (10) (2021) 4759–4771, https://doi.org/10.1007/s12652-021-03184-y.

[54] E. Messner, M. Fediuk, P. Swatek, S. Scheidl, F.-M. Smolle-Jüttner, H. Olschewski, F. Pernkopf, Multi-channel lung sound classification with convolutional recurrent neural networks, Comput. Biol. Med. 122 (2020) 103831, https://doi.org/10.1016/j.compbiomed.2020.103831.https://www.sciencedirect.com/science/article/pii/S0010482520301955

[55] T. Nguyen, F. Pernkopf, Lung sound classification using co-tuning and stochastic normalization, IEEE Trans. Biomed. Eng. 69 (9) (2022) 2872–2882, https://doi.org/10.1109/TBME.2022.3156293.

[56] D. Pessoa, B.M. Rocha, G.-A. Cheimariotis, K. Haris, C. Strodthoff, E. Kaimakamis, N. Maglaveras, I. Frerichs, P. de Carvalho, R.P. Paiva, Classification of electrical impedance tomography data using machine learning. 2021 43rd Annual International Conference of the IEEE Engineering in Medicine & Biology Society (EMBC), 2021, pp. 349–353, https://doi.org/10.1109/EMBC46164.2021.9629961.

[57] N. Vahabi, R. Yerworth, M. Miedema, A. van Kaam, R. Bayford, A. Demosthenous, Deep analysis of EIT dataset to classify apnea and non-apnea cases in neonatal patients, IEEE Access 9 (2021) 25131–25139, https://doi.org/10.1109/ACCESS.2021.3056558.

[58] N. Strodthoff, C. Strodthoff, T. Becher, N. Weiler, I. Frerichs, Inferring respiratory and circulatory parameters from electrical impedance tomography with deep recurrent models, IEEE J Biomed Health Inform 25 (8) (2021) 3105–3111, https://doi.org/10.1109/JBHI.2021.3059016.

[59] Littmann, 3m littmann electronic stethoscope model 3200 user manual, [Accessed 02-Feb-2023], https://multimedia.3m.com/mws/media/594115O/3m-littmann-electronic-stethoscope-model-3200-user-manual.pdf.

[60] L.M.T. Jesus, A. Barney, R. Santos, J. Caetano, J. Jorge, P.S. Couto, Universidade de Aveiro's voice evaluation protocol. Interspeech 2009, ISCA, ISCA, 2009, pp. 971–974, https://doi.org/10.21437/Interspeech.2009-289.https://www.isca-speech.org/archive/interspeech_2009/jesus09_interspeech.html

[61] R. Gravina, P. Alinia, H. Ghasemzadeh, G. Fortino, Multi-sensor fusion in body sensor networks: state-of-the-art and research challenges, Information Fusion 35 (2017) 68–80, https://doi.org/10.1016/j.inffus.2016.09.005.https://www.sciencedirect.com/science/article/pii/S156625351630077X

[62] A. Adler, J.H. Arnold, R. Bayford, A. Borsic, B. Brown, P. Dixon, T.J. Faes, I. Frerichs, H. Gagnon, Y. Gärber, B. Grychtol, G. Hahn, W.R. Lionheart, A. Malik, R.P. Patterson, J. Stocks, A. Tizzard, N. Weiler, G.K. Wolf, GREIT: A unified approach to 2D linear EIT reconstruction of lung images, Physiol Meas 30 (6) (2009), https://doi.org/10.1088/0967-3334/30/6/S03.

[63] A. Adler, W.R. Lionheart, Uses and abuses of EIDORS: an extensible software base for EIT, Physiol Meas 27 (5) (2006), https://doi.org/10.1088/0967-3334/27/5/S03.

[64] B.M. Rocha, D. Pessoa, A. Marques, P. Carvalho, R.P. Paiva, Automatic classification of adventitious respiratory sounds: a (un)solved problem? Sensors 21 (1) (2021) https://doi.org/10.3390/s21010057.https://www.mdpi.com/1424-8220/21/1/57

[65] O. Lartillot, P. Toiviainen, Mir in matlab (ii): A toolbox for musical feature extraction from audio, 2007, pp. 127–130.

[66] J. Snoek, H. Larochelle, R.P. Adams, Practical bayesian optimization of machine learning algorithms. Proceedings of the 25th International Conference on Neural Information Processing Systems - Volume 2, in: NIPS'12, Curran Associates Inc., Red Hook, NY, USA, 2012, p. 29512959.

[67] A. Madhu, S. Kumaraswamy, Data augmentation using generative adversarial network for environmental sound classification. 2019 27th European Signal Processing Conference (EUSIPCO), 2019, pp. 1–5, https://doi.org/10.23919/EUSIPCO.2019.8902819.

[68] I. Frerichs, Z. Zhao, M. Dai, F. Braun, M. Proença, M. Rapin, J. Wacker, M. Lemay, K. Haris, G. Petmezas, A. Cheimariotis, I. Lekka, N. Maglaveras, C. Strodthoff, B. Vogt, L. Lasarow, N. Weiler, D. Pessoa, B. Machado Rocha, P. de Carvalho, R. P. Paiva, A. Adler, Chapter 6 - Respiratory image analysis, in: R.P. Paiva, P. de Carvalho, V. Kilintzis (Eds.), Wearable Sensing and Intelligent Data Analysis for Respiratory Management, Academic Press, 2022, pp. 169–212, https://doi.org/10.1016/B978-0-12-823447-1.00001-4.

[69] C. Jácome, J. Ravn, E. Holsbø, J.C. Aviles-Solis, H. Melbye, L. Ailo Bongo, Convolutional neural network for breathing phase detection in lung sounds, Sensors 19 (8) (2019), https://doi.org/10.3390/s19081798.https://www.mdpi.com/1424-8220/19/8/1798

[70] E. Comission, CORDIS | European Commission — cordis.europa.eu, 2022, (https://cordis.europa.eu/project/id/825572). [Accessed 21-Mar-2023].